TRANSITION FROM AN ANTIFERROMAGNETIC STATE TO A WEAKLY FERROMAGNETIC STATE IN A MAGNETIC FIELD

N. M. KREĬNES

Institute of Physics Problems, Academy of Sciences, U.S.S.R.

Submitted to JETP editor October 25, 1960

J. Exptl. Theoret. Phys. (U.S.S.R.) 40, 762-774 (March, 1961)

The dependence of the magnetic moment of anhydrous cobalt sulfate on temperature and field strength is studied in detail for different crystallographic directions. For the c axis the temperature dependence has been determined for the critical field in which the transition occurs from the antiferromagnetic to the ferromagnetic state. In order to account for the anomalous magnetic properties observed in $CoSO_4$ and previously in $CuSO_4$, the thermodynamic potential is analyzed for the D_{2h}^{16} symmetry group to which the investigated compounds belong. The rapid increase of the susceptibility anisotropy near T_N for $T > T_N$ and the anomalously large value of $\chi_\perp$ below T_N are explained qualitatively.

1. INTRODUCTION

INVESTIGATIONS of the magnetic properties of polycrystalline anhydrous sulfates of Ni^{++}, Co^{++}, Fe^{++}, and Cu^{++}[1,2] have shown that all these compounds are antiferromagnetic. The temperature dependence of the susceptibility of $CoSO_4$ and $CuSO_4$ (Fig. 1 in reference 1 and Fig. 3 in reference 2) exhibits an anomalous increase near the respective transition points in the paramagnetic region.

Single crystals of the same compounds were used in magnetic studies for the purpose of investigating the anomaly in detail. The results obtained for $CuSO_4$, which have been reported in reference 3, show that the sharp rise of the susceptibility above the transition point T_N and its anomalously large value below T_N are observed only for $\chi_\perp$, while $\chi_\parallel$ exhibits ordinary behavior. Preliminary results for a $CoSO_4$ single crystal have also been published,[4] showing that the transition to the antiferromagnetic state is anomalous only along the c axis. At $T = 4.2°K$ anomalous dependence of the magnetic moment on the applied field is observed along the c axis; this is associated with a transition from the antiferromagnetic to the ferromagnetic state. The fact that the maximum spontaneous magnetic moment in $CoSO_4$ is $\sim 30\%$ of the nominal moment calculated assuming complete freezing of orbital moments, and the small value of the critical field required for the transition to ferromagnetism, exclude the possibility that the observed transition in a field can be attributed to the complete destruction of antiferromagnetic ordering.

The present paper reports a more detailed experimental investigation of the anomaly in $CoSO_4$ from 1.3 to 15°K. It is also shown that the anomalies for $CoSO_4$ and $CuSO_4$ above T_N are associated with the fact that in anhydrous sulfates antiferromagnetic ordering combined with weak ferromagnetism can be established.

2. $CoSO_4$ SAMPLES AND MEASUREMENTS

The magnetic properties of $CoSO_4$ single crystals were investigated. The samples were prepared by evaporating a solution of cobalt sulfate in molten ammonium sulfate.*[3] The growth process of $CoSO_4$ crystals is more reliable than that of $CuSO_4$ crystals; the process requires 8 to 10 hours at 430° C. The $CoSO_4$ crystals are dark violet and are very well faceted, so that they can be oriented by face reflections. They are also less hygroscopic than $CuSO_4$. However, in time a transition to a different crystal modification occurs accompanied by color change from dark violet to pink and by crumbling to a powder. The magnetic properties of the powder differ from those of the crystals, but we have not studied the former in detail.

Our largest $CoSO_4$ samples weighed 1.0 to 1.5 mg, with linear dimensions up to 1 mm. These crystals were rectangular bipyramids. In most

*The author is greatly indebted to N. N. Mikhaĭlov for his assistance in preparing $CoSO_4$ single crystals.

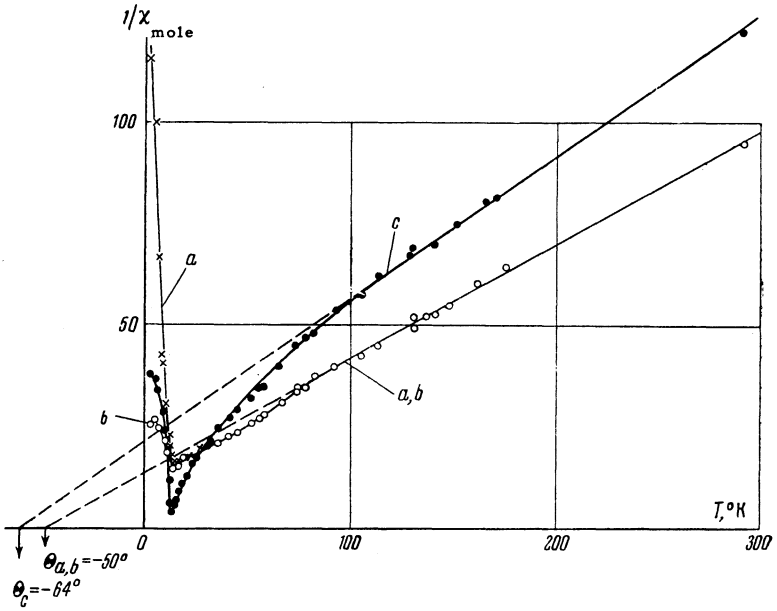

FIG. 1. Temperature dependence ot the reciprocal molar susceptibility of $CoSO_4$ along the a, b, and c axes.

instances the two pyramids were shifted relative to each other along the a axis. The structure of anhydrous cobalt sulfate has not yet been investigated thoroughly. Hammel's[5] x-ray study of powdered samples revealed an orthorhombic lattice with four molecules in the unit cell. The lattice constants are a = 8.46 A, b = 6.66 A, and c = 4.65 A.* Recent x-ray studies of $CuSO_4$ and $ZnSO_4$ single crystals[6] showed that these compounds both belong to the D_{2h}^{16} space group. We thus have a basis for the hypothesis that $CoSO_4$ belongs to the same symmetry group.

The triaxial character of our $CoSO_4$ crystals was confirmed goniometrically. The b axis passes through the vertex of the pyramid perpendicular to its base; the a and c axes are parallel to the edges of the base. At the vertex opposite faces form angles of 65° and 70°. These angles are in best agreement with the assumption that the faces are (210) and (011) planes. The c axis is then parallel to the faces forming the 65° angle, and the a axis is perpendicular to the c axis.

Our magnetic measurements were obtained with the apparatus described in reference 7. The range of magnetic field strengths was broadened by the use of pole pieces such as those employed by Sucksmith.[8] The magnetic field at the second maximum of $H\partial H/\partial z$ was thus increased to 18 koe. However, since $H\partial H/\partial z$ in this region is considerably smaller than at the upper maximum, the sensitivity of the apparatus was somewhat reduced. Small moments were thus measured less accurately. As a result, at high temperatures (above ~ 60° K), where the magnetic moments are small, the accuracy of relative measurements was 5 to 6%; at low temperatures it was 2%.

We studied a few $CoSO_4$ single crystals weighing from 0.5 to 1.5 mg. A crystal with proper orientation (attained by x-ray or goniometric means) was attached to the quartz rod of the suspension with BF cement. The accuracy of orientation and suspension was 2 to 3°. Magnetic susceptibility was measured along all three crystal axes at temperatures from 1.3 to 300° K.

At all temperatures the susceptibility is field-independent up to ~ 4 koe. Figure 1 shows the temperature dependence of the reciprocal molar susceptibility of $CoSO_4$. From 300° down to 14 — 18° K the susceptibilities along the a and b axes coincide. In almost this entire temperature range $\chi_{a,b} > \chi_c$; the sign of the susceptibility anisotropy is reversed only at T ≈ 27° K. The Curie-Weiss law is obeyed for both directions in the approximate range 100 — 300° K. Along the c axis we have the law $\chi = 2.89/(T+64)$ with the g-factor 2.48; along the b axis we have $\chi = 3.59/(T+50)$ with the g-factor 2.77.

Figure 1 in reference 4, which gives the temperature dependence of the molar susceptibility of $CoSO_4$ from 1.3 to 70° K, shows that the maximum susceptibility along all three axes is attained at T_N = 12° K. The anisotropy increases sharply and there is a very sharp susceptibility peak along the c axis at this temperature. Below 12° the susceptibility differs along the three axes. It is interesting that at T → 0° K the susceptibility does not

*In the present paper the notation for the $CoSO_4$ lattice constants differs from that in reference 1 and 5, so that the orientation of $CoSO_4$ can correspond to that of $CuSO_4$ given in reference 6.

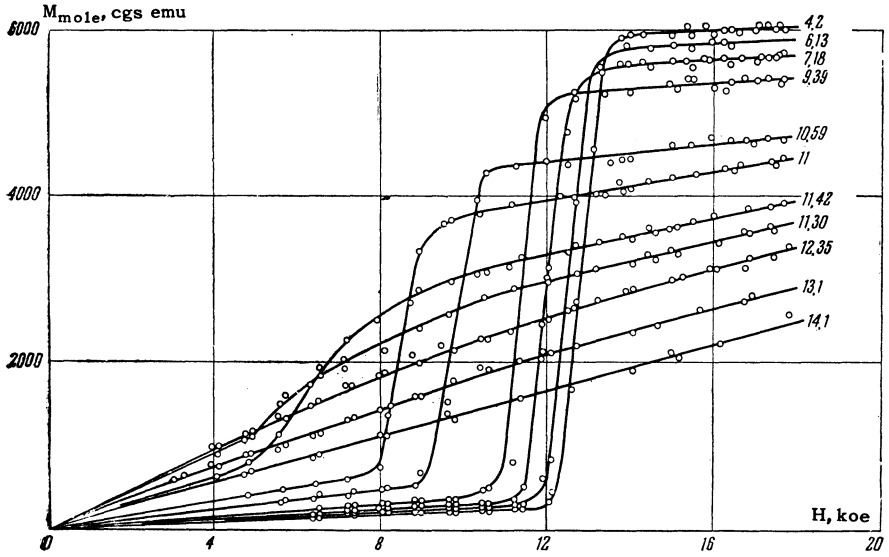

FIG. 2. Magnetic moment of $CoSO_4$ along the c axis vs magnetic field at different temperatures (indicated in °K at the end of each curve).

approach exactly zero along any one of the axes.

The results obtained in large fields parallel to the c axis are of greatest interest. Although susceptibility along the a and b axes is field-independent up to 18 koe, magnetic properties along the c axis exhibit a sharp anomaly in the antiferromagnetic region. Figure 2 shows the field dependence of the molar magnetic moment along this axis at different temperatures. Up to a value H_{cr} the moment increases linearly with the field. This is followed by a sharp increase of the moment up to a value M_S, after which it increases slowly with H. The M(H) curves and M_S and H_{cr} depend on temperature; as the temperature increases the transition region is broadened, while H_{cr} and M_S are diminished.

Slight nonlinearity in the field dependence of the magnetic moment is also observed above the antiferromagnetic transition point and disappears completely only at 14° K. The sharpest field-dependent increase of the moment occurs at the lowest temperatures; below 4° K the M(H) curves coincide within error limits. The moment increases by a factor of almost 20 (from 300 to 5900 cgs emu) as the field changes from 12 to 13.2 koe. We obtained a maximum moment of 6000 cgs emu.

The value of the maximum moment diminishes with time; in our samples the change amounted to ~ 10% after two weeks. This reduction is apparently associated with a partial transition to a different crystal modification.

The temperature variation of the magnetic moment is shown in Fig. 3. The peak of the M(T) curve is seen to shift toward lower temperatures as the field strength increases. The peak is shifted by 6° K with a field increase of ~ 9 koe. The M(T) curves have no peak in fields $\gtrsim$ 14 koe and are saturated at low temperatures.

Figure 4 shows how the force acting on a sample depends on the magnetic field direction in different fields at T = 4.2° K. Curve 1 pertains to the field below H_{cr}, curve 2 to the transition region, and curve 3 to the maximum field. Curve 3 exhibits flat-topped peaks.

3. THEORY

Anomalous increase of the magnetic moment as the field is strengthened, similar to that observed for $CoSO_4$, had been observed earlier by Shalyt[9] in polycrystalline $FeCl_2$, and by Bizette et al.[10] in a single crystal. However, $FeCl_2$ is a layer-type antiferromagnet with a strong ferromagnetic intralayer interaction and weak antiferromagnetic interaction between layers; this is revealed by the ferromagnetic sign of the constant Θ in the Curie-Weiss law. The ferromagnetic moment is here associated with flipping of the moments in layers,[11] which is entirely natural for the given structure even in weak fields. Similar magnetic behavior has been observed in the intermetallic compound $MnAu_2$[12] and in the rare-earth elements Dy, Ho, and Er.[13-15]

$CoSO_4$ is the first ionic crystal having an antiferromagnetic sign of Θ where destruction of the initial antiferromagnetic structure was observed in a relatively weak field ($\mu H \ll kT$). We shall show that this effect and the anomaly observed earlier in the temperature variation of $CuSO_4$ susceptibility[3] are associated with the fact that antiferromagnetic ordering combined with weak ferromagnetism can be established in anhydrous sulfates. We shall apply the theory of second-

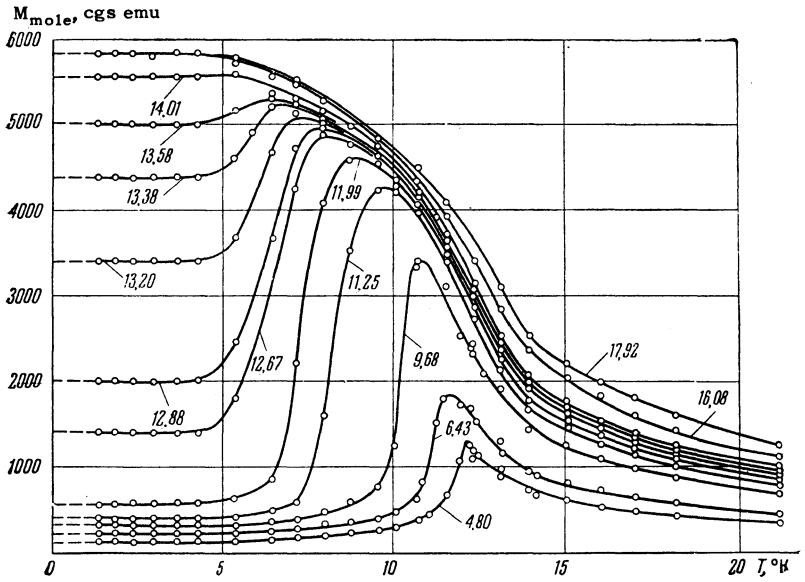

FIG. 3. Magnetic moment of $CoSO_4$ along the c axis vs temperature in different fields (indicated in kilo-oersteds along the curves).

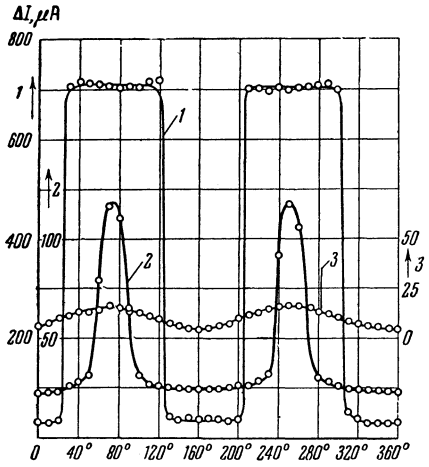

FIG. 4. Force acting on a sample vs angle between the magnetic field and c axis, in different fields. 1 – H = 17.9 koe; 2 – H = 12.7 koe; 3 – H = 8 koe.

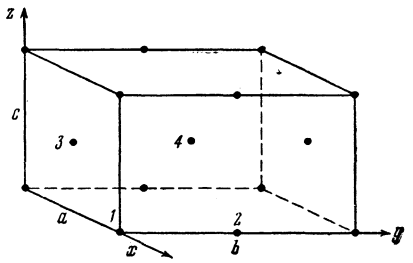

FIG. 5. Metallic ions in sulfate unit cell. For $CuSO_4$ a = 8.39 A, b = 6.69 A, c = 4.83 A; for $CoSO_4$ a = 8.46 A, b = 6.66 A, and c = 4.65 A.

order phase transitions to this problem, as has been done by Dzyaloshinskii.[16]

$CuSO_4$ crystals possess the symmetry of the D_{2h}^{16} space group, with four metallic ions in each unit cell arranged as shown in Fig. 5. We introduce the vectors $\mathbf{m}$, $\mathbf{l}_1$, $\mathbf{l}_2$, $\mathbf{l}_3$, defined by

$$\mathbf{m} = \mathbf{s}_1 + \mathbf{s}_2 + \mathbf{s}_3 + \mathbf{s}_4,$$
$$\mathbf{l}_1 = \mathbf{s}_1 - \mathbf{s}_2 - \mathbf{s}_3 + \mathbf{s}_4, \quad \mathbf{l}_2 = \mathbf{s}_1 - \mathbf{s}_2 + \mathbf{s}_3 - \mathbf{s}_4,$$
$$\mathbf{l}_3 = \mathbf{s}_1 + \mathbf{s}_2 - \mathbf{s}_3 - \mathbf{s}_4. \qquad (1)$$

Here $\mathbf{s}_1$, $\mathbf{s}_2$, $\mathbf{s}_3$, $\mathbf{s}_4$ are the respective spins of the four ions. $\mathbf{m}$ is obviously the mean magnetic moment of the unit cell, and $\mathbf{l}_1$, $\mathbf{l}_2$, $\mathbf{l}_3$ are antiferromagnetic vectors corresponding to the different possible magnetic structures.

When the representation of the D_{2h}^{16} group formed by the twenty vectors in (1) is transformed into irreducible representations we find that this symmetry group permits nine types of antiferromagnetic ordering, three of which are purely antiferromagnetic (A), while the other six possess weak ferromagnetism (AWF). The types of ordering are listed in the table.

When the irreducible representations transforming the vectors in (1) are known, the most general expansion of the thermodynamic potential

Types of antiferromagnetic ordering* permitted by the D_{2h}^{16} space group

State	l_1	l_2	l_3	m	State	l_1	l_2	l_3	m
A_1	l_{1x}				AWF_{1y}	l_{1z}			m_y
A_2		l_{2z}			AWF_{2y}		l_{2x}		m_y
A_3			l_{3y}		AWF_{1z}	l_{1y}			m_z
AWF_{2x}		l_{2y}		m_x	AWF_{3z}			l_{3x}	m_z
AWF_{3x}			l_{3z}	m_x					

*The type of order is indicated by the subscripts 1, 2, 3; the spin direction is indicated by x, y, z.

to second-order terms is easily obtained, as follows:

$$\Phi = \tfrac{1}{2} A_1 l_1^2 + \tfrac{1}{2} A_2 l_2^2 + \tfrac{1}{2} A_3 l_3^2 + \tfrac{1}{2} Bm^2 + \tfrac{1}{2} a_1' l_{1x}^2 + \tfrac{1}{2} a_1'' l_{1y}^2 + \tfrac{1}{2} a_2' l_{2x}^2 + \tfrac{1}{2} a_2'' l_{2y}^2 + \tfrac{1}{2} a_3' l_{3x}^2 + \tfrac{1}{2} a_3'' l_{3y}^2 + \tfrac{1}{2} b_1 m_x^2 + \tfrac{1}{2} b_2 m_y^2 + \beta_1 m_x l_{2y} + \beta_2 m_x l_{3z} + \beta_1' m_y l_{1z} + \beta_2' m_y l_{2x} + \beta_1'' m_z l_{1y} + \beta_2''' m_z l_{3x} + \gamma_1 l_{2y} l_{3z} + \gamma_2 l_{1z} l_{2x} + \gamma_3 l_{1y} l_{3x} + \gamma_4 l_{1x} l_{2z} + \gamma_5 l_{2z} l_{3y} + \gamma_6 l_{1x} l_{3y}. \quad (2)$$

The last six terms in this expansion of Φ show that none of the states listed above is realized in its pure form, but each one is always accompanied by some admixture. We shall hereafter assume this effect to be negligibly small, without affecting our results qualitatively.

The foregoing types of ordering for the D_{2h}^{16} group were first obtained by Bozorth,[17] who used them to account for the ferromagnetism of orthoferrites. Turov and Naĭsh[18] made a detailed study of the magnetic properties of orthoferrites in external fields, based on an analysis of (2). However, unlike these investigators, we shall assume that in the absence of a magnetic field one of the pure antiferromagnetic states (for definiteness, A_2) is realized below the transition point. We shall be interested in determining whether the application of a magnetic field induces other states possessing weak ferromagnetism.

A field perpendicular to and a field parallel to the direction of antiferromagnetic ordering present two qualitatively different cases. In the first case ($H \perp Oz$) the field induces the AWF_{2x} and AWF_{2y} states with weak ferromagnetism but without reordering of the spins. We can therefore put $l_1 = l_3 = 0$ and write the potential in the considerably simpler form

$$\tilde{\Phi} = \tfrac{1}{2} Al^2 + \tfrac{1}{2} Bm^2 + \tfrac{1}{2} a_1 l_x^2 + \tfrac{1}{2} a_2 l_y^2 + \tfrac{1}{2} b_1 m_x^2 + \tfrac{1}{2} b_2 m_y^2 + \beta_1 m_x l_y + \beta_2 m_y l_x + \tfrac{1}{4} Cl^4 - \mathbf{mH}. \quad (3)$$

Here the most important fourth-order exchange term has been taken into account.

Using the scheme proposed by Borovik-Romanov and Ozhogin,[19] we obtain the following solutions for $\mathbf{m}$ and $\mathbf{l}$:

$$m_x = \frac{H_x}{B+b_1} - \frac{\beta_1 l_y}{B+b_1}, \quad m_y = \frac{H_y}{B+b_2} - \frac{\beta_2 l_x}{B+b_2}, \quad m_z = \frac{H_z}{B};$$

$$l_x = \frac{\beta_2 H_y}{\beta_2^2 - (B+b_2)(A+a_1+Cl^2)},$$

$$l_y = \frac{\beta_1 H_x}{\beta_1^2 - (B+b_1)(A+a_1+Cl^2)},$$

$$l_z(A+Cl^2) = 0, \qquad l^2 = l_x^2 + l_y^2 + l_z^2. \quad (4)$$

The coefficient $A = 0$ at the transition point T_N; near T_N we shall, as usual, assume

$$A = \lambda (T - T_N). \quad (5)$$

It is also useful to introduce two characteristic temperatures:

$$T_1 = T_N - \lambda^{-1}(a_1 - \beta_2^2/(B+b_2)),$$

$$T_2 = T_N - \lambda^{-1}(a_2 - \beta_1^2/(B+b_1)), \quad (6)$$

which determine the ordering energy in the states AWF_{2y} and AWF_{2x}, respectively. It follows from our assumptions regarding the magnitudes and signs of the constants in (3) that $T_N > T_1$ and $T_N > T_2$.

Above the transition point ($T > T_N$) $l_z \equiv 0$. Neglecting Cl^4 and using (6), the equations in (4) finally become

$$m_x = \left[\frac{1}{B+b_1} + \frac{\beta_1^2}{(B+b_1)^2 (T-T_2)\lambda}\right] H_x,$$

$$m_y = \left[\frac{1}{B+b_2} + \frac{\beta_2^2}{(B+b_2)^2 (T-T_1)\lambda}\right] H_y, \quad m_z = \frac{H_z}{B};$$

$$l_x = \frac{\beta_2 H_y}{(B+b_2)\lambda (T_1 - T)}, \quad l_y = \frac{\beta_1 H_x}{(B+b_1)\lambda (T_2 - T)}, \quad l_z = 0. \quad (7)$$

Below the transition point ($T < T_N$) $l_z \neq 0$; consequently, in (4), $A + Cl^2 = 0$ and $l^2 = -A/C$. We then obtain

$$m_x = \frac{H_x}{B + b_1 - \beta_1^2/a_2}, \quad m_y = \frac{H_y}{B + b_2 - \beta_2^2/a_1}, \quad m_z = \frac{H_z}{B};$$

$$l_x = \frac{\beta_2 H_y}{\beta_2^2 - (B+b_2) a_1}, \quad l_y = \frac{\beta_1 H_x}{\beta_1^2 - (B+b_1) a_2}, \quad l_z^2 = l^2 - (l_y^2 + l_x^2). \quad (8)$$

The equations in (7) show that in the given case a magnetic field also induces antiferromagnetic ordering above T_N. It can be seen from (7) that the magnetic moment varies linearly with the field, and that the paramagnetic susceptibility increases sharply as the transition point is approached. Below the transition point the susceptibility is constant and greater in absolute magnitude than in the absence of weak ferromagnetism.

It is shown by (8) that below the transition point an external magnetic field rotates the vector $\mathbf{l}$ (directed along the z axis when $H = 0$) toward the xy plane; l_x and l_y are then proportional to H_y and H_x, respectively. In a certain field H_{cr}, $\mathbf{l}$ lies entirely in the xy plane and l_z vanishes. In the special cases $H = H_x$ and $H = H_y$ the critical fields are

$$H_{cr} = (\beta_1^2 - (B+b_1)a_2) l/\beta_1,$$

$$H_{cr} = (\beta_2^2 - (B+b_2) a_1) l/\beta_2. \quad (9)$$

When l_z vanishes the condition $A + Cl^2 = 0$ [in (4)] is not required, and l can vary with the field. We obtain the following dependence of l_x on H_y near the transition point:

$$l_x = \sqrt{\lambda (T_1 - T)/C} + \beta_2 H_y/2 (B + b_2) \lambda (T_1 - T). \quad (10)$$

Substituting (10) in the expression for m_y in (4), we obtain a relationship that is typical for antiferromagnets possessing weak ferromagnetism:

$$m_y = \sigma + \chi H. \quad (11)$$

At low temperatures in strong fields l becomes large and the expansion (3) cannot be used. However, by expanding in powers of the unit vector γ in the direction of l, we can derive equations similar to (8), (9), and (11).

By comparing the expressions for m_y in (11) and (8) we learn the following. l_x in a weak field H_y is accompanied by a supplementary ferromagnetic moment along the y axis. In fields smaller than H_{ycr} this has the sole effect of increasing the magnetic susceptibility along that axis compared with ordinary paramagnetic susceptibility. In fields greater than H_{ycr}, m_y contains a field-independent term representing a spontaneous ferromagnetic moment. Thus when the field is perpendicular to the direction of antiferromagnetic ordering a state with weak ferromagnetism can arise. The mechanism responsible for this state is associated with the rotation of the antiferromagnetic vector into the plane perpendicular to its original direction.

In the second case, when the field is parallel to the direction of antiferromagnetic ordering, the table shows that simple rotation of the antiferromagnetic vector l_2 cannot produce weak ferromagnetism in this direction. A change of structure and a transition to the state AWF_{1z} ($l_{1y} \neq 0$) or AWF_{3z} ($l_{3x} \neq 0$) are required. The energy of one of these states must differ very little ($\sim 1°K$) from that of the original state A_2. We shall assume that this is true for the state AWF_{1z}.

In accordance with the foregoing assumptions and using the notation $l_{1y} = l_1$ and $l_{2z} = l_2$, the potential (2) can be expressed by

$$\tilde{\Phi} = \tfrac{1}{2}(A_1 + a) l_1^2 + \tfrac{1}{2} A_2 l_2^2 + \tfrac{1}{2} B m_z^2 - \beta m_z l_1 + \tfrac{1}{4} C_1 l_1^4 + \tfrac{1}{4} C_2 l_2^4 + \tfrac{1}{2} D l_1^2 l_2^2 - m_z H_z. \quad (12)$$

The principal fourth-order exchange terms have here been taken into account. By minimizing $\tilde{\Phi}$ we obtain two solutions:

$$l_2 = 0, \qquad \frac{\beta}{l_1 B} H_z = C_1 l_1^2 + \lambda_1 (T - T_1), \qquad m_z = \frac{H_z + \beta l_1}{B};$$
$$l_2^2 = -[\lambda (T - T_N) + D l_1^2] C_2^{-1}, \quad (13a)$$

$$\frac{\beta}{l_1 B} H_z = C_1 l_1^2 \left(1 - \frac{D^2}{C_1 C_2}\right) + \lambda_1 (T - T_1) - \frac{D}{C_2} \lambda (T - T_N),$$
$$m_z = \frac{H_z + \beta l_1}{B}, \quad (13b)$$

where

$$\lambda (T - T_N) = A_2, \qquad \lambda_1 (T - T_1) = A_1 + a - \beta^2/B. \quad (14)$$

Equation (13a) shows that the result for the paramagnetic region is entirely analogous to that obtained for perpendicular fields. We therefore have

$$m_z = [1/B + \beta^2/B (T - T_1)\lambda_1] H_x. \quad (15)$$

The complexity of the foregoing equations necessitated a graphical method of solution for $T < T_N$. With empirically determined coefficients in Eqs. (13a) and (13b) and making certain assumptions concerning the region in which solutions exist, we obtained graphically $l_1(H)$ at different temperatures and $l_1(T)$ in different fields (Figs. 6 and 7), as well as the region in which the state A_2 ($l_2 \neq 0$) exists for different fields and temperatures. Figure 7 shows that below $T = 11°K$ there exists for each temperature a critical field in which the value of l_1 jumps discontinuously. l_2 vanishes at the same point, i.e., the critical field transforms the material from an ordered mixture of A_2 ($l_2 \neq 0$) and AWF_{1z} ($l_1 \neq 0$) to a pure AWF_{1z} ($l_1 \neq 0$) state possessing weak ferromagnetism.

At temperatures from T_N (11.7°) to T_1 (11°) in fields from 0 to 4.5 koe the state A_2 is reached by a second-order transition; the $l_1(H)$ and $l_1(T)$ curves exhibit kinks but no jumps. Below T_1 in fields above 4.5 koe, A_2 is reached by a first-order transition; the $l_1(H)$ and $l_1(T)$ curves exhibit jumps in these regions. It should be noted that in this case $\chi_{||}$ will not approach zero when

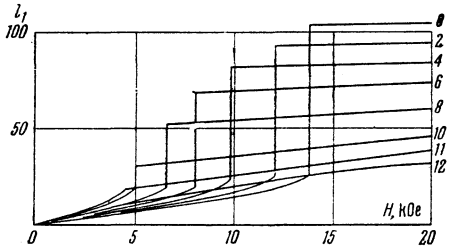

FIG. 6. Field dependence of the antiferromagnetic vector l_1 at different temperatures (indicated in °K at the end of each curve).

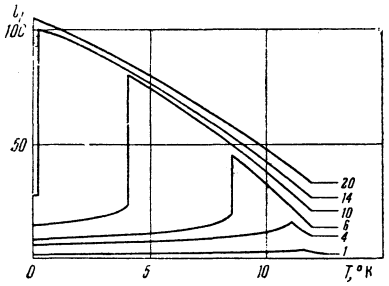

FIG. 7. Temperature dependence of the antiferromagnetic vector l_1 in different fields (indicated in kilo-oersteds at the end of each curve).

$T \to 0°K$ even in weak fields. This follows readily from the potential (12) without fourth-order terms at low temperatures and $\mathbf{l}_1^2 + \mathbf{l}_2^2 + \mathbf{m}^2 = \text{const}$.

For the case $\mathbf{H} \parallel Oz$ we were forced to make a number of assumptions regarding the magnitudes of the expansion coefficients. The results therefore represent only one of the possible special cases in the behavior of the given crystals. Reordering of the structure is also possible in the case $\mathbf{H} \perp Oz$. Since the expansion (12) is valid only around T_N, the theoretical curves in Figs. 6 and 7 can be regarded as only very rough extrapolations far from the transition point.

Our theoretical results lead to the following conclusion. A field can induce weak ferromagnetism even in a crystal that is purely antiferromagnetic in the absence of the field. This can occur only if the symmetry group of the crystal permits weak ferromagnetism in zero field in addition to the pure antiferromagnetic state. In this case increasing susceptibility will always be observed along the direction permitting weak ferromagnetism as T_N is approached from higher temperatures.

The foregoing formulas hold true around but not too near T_N, according to the limitations introduced by Borovik-Romanov and Ozhogin.[19] The anomalies predicted by the formulas will be observed only for sufficiently large values of the constant β, which is responsible for weak ferromagnetism. Closeness of T_i to T_N is another requirement.

4. DISCUSSION OF RESULTS

The results obtained for the antiferromagnetic compounds $CoSO_4$ and $CuSO_4$ will now be discussed and compared with the theory.

1. Near the transition point where $T > T_N$ the susceptibility increases sharply along the c axis for $CoSO_4$ (Fig. 1 in reference 4) and along the a and b axes for $CuSO_4$ (Fig. 3 in reference 3). $\chi_a = \chi_b$ for the latter. The preceding theoretical discussion shows that this behavior can be accounted for by field-induced antiferromagnetic ordering near T_N. The temperature dependence of the susceptibility for this case is given by (7) or (15). For the purpose of comparing the experimental results with these equations we have plotted the temperature variation of $1/\Delta\chi$ for $CuSO_4$ and $CoSO_4$ (Fig. 8). For the former compound $\Delta\chi$ represents the difference $\chi_\perp - \chi_\parallel$, for the latter it represents $\chi_c - \chi^*$, where χ^* is an extrapolation of the Curie-Weiss law for χ_c. χ^* is somewhat arbitrary in the case of $CoSO_4$, since the Curie-Weiss law is ordinarily not observed by Co^{++} ions at low temperatures. However, the resulting error will not be very large since, first, $\Delta\chi \gg \chi^*$, and, secondly, χ^* should not change appreciably in the given small temperature interval.

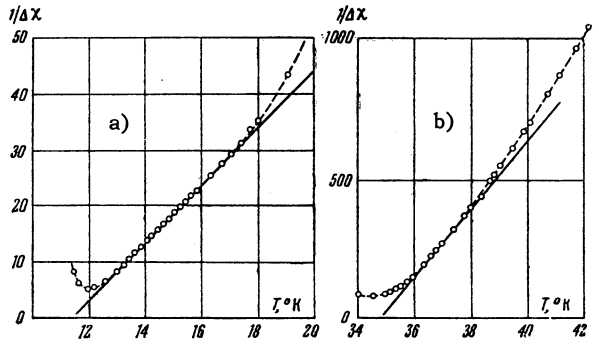

FIG. 8. Temperature dependence of $1/\Delta\chi$ near T_N. a – for $CoSO_4$; b – for $CuSO_4$.

The linear portions of the curves in Fig. 8 indicate the qualitative agreement of the experimental results with theoretical formulas over a 2° interval for $CuSO_4$ and a 4° interval for $CoSO_4$. This makes it possible to determine the temperature T_1 associated with the energy of the corresponding weakly ferromagnetic states that induce the anomalous rise of χ. Taking $T_N = 12°$ for $CoSO_4$ and 35.5° for $CuSO_4$, we obtain $T_N - T_1 = 0.6°$ for $CoSO_4$ and $T_N - T_1 = 0.8°K$ for $CuSO_4$. The experimental curves of $\chi_\parallel$ and $\chi_\perp$ for $CuSO_4$ exhibit peaks at different temperatures. It was reasonable to take the temperature for the maximum of $\chi_\parallel$ as T_N, since according to (10) the maximum of $\chi_\perp$ must depend strongly on the applied field, as has actually been observed experimentally.[2,3]

The results obtained at temperatures above T_N thus show that, although both substances perform a transition to pure antiferromagnetism at T_N, in each of them one of the states with weak ferromagnetism differs very little energetically ($< 1°K$) from pure antiferromagnetism. The behavior for $T < T_N$ must be considered in determining the actual states.

2. In the case of $CuSO_4$ (Fig. 3 in reference 3) the temperature dependence of χ_c below T_N indicates that the c axis is the axis of easy magnetization, and that the transition to the state A_2 therefore occurs when $H = 0$. The anomalous behavior of $\chi_\perp$ in $CuSO_4$ can therefore be accounted for by a mechanism for the generation of weak ferromagnetism, associated with rotation of the antiferromagnetic vector in a field. In these fields below H_{cr}, $\chi_\perp$ should have an unusually large value [see Eq. (8)]; this was observed experimentally.

The experimental data for $CuSO_4$ enable us to estimate some expansion coefficients of the thermodynamic potential, as well as the critical field, from the formula $\frac{1}{2}\chi H_{cr}^2 = k(T_N - T_1)$. We obtain $B = 270$, $\beta^2/a = 188$, and $H_{cr} \approx 100$ koe.

The observed behavior of the susceptibility of $CuSO_4$ is similar to that of CoF_2.[20,21] Dzyaloshinskii[22] has shown that the symmetry group of CoF_2 allows a weakly ferromagnetic state. We can therefore assume that CoF_2 is also subject to a mechanism producing weak ferromagnetism, associated with the rotation of the antiferromagnetic vector in a field.

3. In the case of $CoSO_4$ we do not arrive at such a definite conclusion regarding the direction of spontaneous magnetization. The two most essential facts for $T < T_N$ are: a) χ does not approach zero along any axis when $T \to 0$, and b) the magnetic moment along the c axis increases sharply at a certain strength of the external field. From a comparison with item 2) we conclude that $CoSO_4$ is in state A_2 at $H = 0$. One of the weakly ferromagnetic states AWF_{1z} or AWF_{3z} should therefore result when a magnetic field is applied along a magnetization direction of the sublattices.

The available experimental data do not enable us to determine what state actually exists. The foregoing conclusions regarding the states of $CoSO_4$ are confirmed by the good qualitative agreement between experiment (Figs. 2 and 3) and theory (Figs. 6 and 7). It should be noted that, since l_1 and m_z are related as in (13), the field and temperature dependences of m_z are represented by the curves in Figs. 6 and 7. It must be remembered that the theoretical curves are only very rough extrapolations at a large distance from the transition point.

Figure 9 gives the temperature dependence of H_{cr}, which for definiteness was taken to be the field at the upper knee of the M(H) curves in Fig. 2. According to the foregoing discussion these curves depict the transition from the mixture of states A_2 and AWF_{1z} to the state AWF_{1z}. $m_{max}H_{cr}$ must obviously be of the order of the energy difference between A_2 and AWF_{1z}. $T_N - T_1 = 0.8°K$ obtained in this manner agrees well with the temperature dependence of χ in the paramagnetic region. This result is $\sim 7\%$ of the total exchange energy; as pointed out in our introduction, this excludes the possibility of accounting for the observed transition in a field as resulting from complete destruction of antiferromagnetic ordering. Figure 9 shows that the temperature dependence of H_{cr} over a broad temperature range is represented by the empirical law

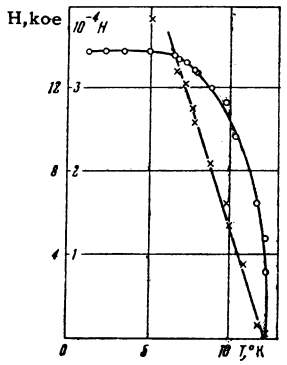

FIG. 9. Temperature dependence of H_{cr}. o – the function $H_{cr}(T)$ (left-hand scale); × – the function $H_{cr}^4(T)$ (right-hand scale).

$$(H_{cr}/H_{0cr})^4 = 1 - \alpha T. \quad (16)$$

Two conclusions result from the rotation diagrams in Fig. 4. First, the ferromagnetic moment disappears at angles where the projection of the external field on the c axis equals H_{cr}. Secondly, the broad flat peaks of the curves apparently indicate that the ferromagnetic moment can form an appreciable angle with the c axis.

The results for $CoSO_4$ show that although the crystal structure of $CoSO_4$ is unknown, the theoretical results derived from a consideration of space group D_{2h}^{16} are in good agreement with experimental findings for this substance.

In conclusion the author wishes to thank A. S. Borovik-Romanov for his continued interest and guidance. The author is also grateful to Academician P. L. Kapitza for his continued interest, to I. E. Dzyaloshinskii for several valuable suggestions and helpful discussions, and to V. I. Kolokol'nikov for assistance with the measurements.

[1] Borovik-Romanov, Karasik, and Kreĭnes, JETP **31**, 18 (1956), Soviet Phys. JETP **4**, 109 (1957).

[2] A. S. Borovik-Romanov and N. M. Kreĭnes, JETP **33**, 1119 (1957), Soviet Phys. JETP **6**, 826 (1958).

[3] N. M. Kreĭnes, JETP **35**, 1391 (1958), Soviet Phys. JETP **8**, 972 (1959).

[4] A. S. Borovik-Romanov and N. M. Kreĭnes, JETP **35**, 1053 (1958), Soviet Phys. JETP **8**, 734 (1959).

[5] F. Hammel, Ann. chim. **11**, 247 (1939).

[6] P. A. Kokkoros and P. J. Rentzeperis, Acta Cryst. **11**, 361 (1958).

[7] A. S. Borovik-Romanov, Dissertation, Institute of Physics Problems, Acad. Sci. U.S.S.R., Moscow, 1959.

[8] W. Sucksmith, Proc. Roy. Soc. (London) **A170**, 551 (1939).

[9] S. S. Shalyt, JETP **15**, 246 (1945).

[10] Bizette, Terrier, and Tsai, Compt. rend **243**, 895 (1956).

[11] Wilkinson, Cable, Wollan, and Koehler, Phys. Rev. **113**, 497 (1959).

[12] A. Y. P. Meyer and P. Taglang, Compt. rend. **239**, 961 (1954).

[13] Behrendt, Legvold, and Spedding, Phys. Rev. **109**, 1544 (1958).

[14] Rhodes, Legvold, and Spedding, Phys. Rev. **109**, 1547 (1958).

[15] Elliott, Legvold, and Spedding, Phys. Rev. **100**, 1595 (1955).

[16] I. E. Dzyaloshinskii, JETP **32**, 1547 (1957), Soviet Phys. JETP **5**, 1259 (1957).

[17] R. M. Bozorth, Phys. Rev. Letters **1**, 362 (1958).

[18] E. A. Turov and V. E. Naĭsh, Физика металлов и металловедение (Physics of Metals and Metallography) **9**, 10 (1960).

[19] A. S. Borovik-Romanov and V. I. Ozhogin, JETP **39**, 27 (1960), Soviet Phys. JETP **12**, 18 (1961).

[20] J. W. Stout and L. M. Matarrese, Revs. Modern Phys. **25**, 338 (1953).

[21] Astrov, Borovik-Romanov, and Orlova, JETP **33**, 812 (1957), Soviet Phys. JETP **6**, 626 (1958).

[22] I. E. Dzyaloshinskii, JETP **33**, 1454 (1957), Soviet Phys. JETP **6**, 1120 (1958).

Translated by I. Emin
124